SUPPLEMENTAL MATERIALS

Supplemental Methods

Supplemental Results

Supplemental References

SUPPLEMENTAL METHODS

Histopathologic assessment of primary lung specimens by chemotherapy response criteria

Hematoxylin and eosin (H&E)-stained slides of the primary lung tumor and lymph node resection specimens were evaluated and staged according to the AJCC-pTNM system, 7th edition [1]. Post-treatment specimens were scored for %cRVT, as described previously, and summarized in Table 2 [2]. Patients with no (0%) RVT are pathologic complete responders (pCR), and those with ≤10% cRVT are classified as cMPR. As lymph nodes are not specifically addressed by chemotherapy pathologic response criteria [2, 3], they were assessed as being positive or negative for tumor deposits, and the diameter of the largest tumor deposit was recorded, per standard AJCC pTNM staging.

Histopathologic assessment of primary lung specimens for immune-mediated response

Histopathologic analysis of the primary tumor resection specimen was conducted to nominate candidate immune and non-immune features potentially related to immunotherapeutic response, many of which have also been studied in the context of chemotherapy [2, 4, 5]. Tumor infiltrating lymphocytes (TIL) and associated macrophages were scored as previously described [6]. The presence or absence of lymphoid aggregates (≥100 lymphocytes without a germinal center) and tertiary lymphoid structures (≥100 lymphocytes with a germinal center and high endothelial venules, TLS) was also noted. Dense plasma cell infiltrates (≥100 plasma cells/high power field (HPF) in at least two HPFs) were scored. Neutrophils in non-necrotic regions of tumor, foamy (lipid-filled) macrophages in interstitial and alveolar locations, hemosiderin-laden macrophages, giant cells, granulomas, cholesterol clefts, and neovascularization were scored as present vs. absent. The percentage surface area of the mass involved by necrosis and fibrosis were each quantified at 5% intervals. The presence of immature or cellular fibrosis and/or paucicellular, mature fibrosis was also recorded. (Also see **Table 1** for feature descriptions.)

The two extremes of the cohort were first compared, i.e., the patients with pCR/cMPR (n=9) and the pathologic non-responders (cNR) (n=4, >90% RVT). Following the nomination of features that potentially differed between pathologic responders and non-responders, all twenty pre- and post-treatment lung tumor specimens were independently scored by two pathologists. Discordant results were adjudicated with a third pathologist.

Quantification of immune-related pathologic response: Reproducibility amongst pathologists

Immune-related pathologic response criteria (irPRC) were then developed, incorporating the regression bed as a major feature (specifically defined by proliferative fibrosis with neovascularization and evidence of immune activation and cell death, detailed in Results section and **Table S1**). In this system, the tumor bed is defined by RVT + necrosis + regression bed. The total percent surface area(s) of each of these three components is estimated across all slides to calculate %irRVT (RVT area/tumor bed area x 100). If multiple foci of residual tumor are present, these are added together for the RVT area, provided they are located in a single tumor bed. Scans of example slides showing the tumor bed (circled in green) and residual viable tumor (circled in blue) can be found at: https://digital.pathology.johnshopkins.edu/repos/578.

Additional pathologic analysis: Immune exclusion

On H&E stain, tumors were assessed for lymphocyte exclusion, defined as an accumulation of lymphocytes in the immediately adjacent peritumoral stroma that fail to infiltrate the neoplastic epithelium. Standard, automated chromogenic CD8 immunostains as well as multiplex immunohistochemistry/immunofluorescence (IHC/IF) (pan-cytokeratin to mark tumor combined with CD8, as previously described) [7] were performed on select cases for illustrative purposes.

SUPPLEMENTAL RESULTS

Comparison of pre- vs. post-anti-PD-1 treatment tumor specimens

When all available pre-/post-treatment paired specimens (n=17) were assessed, the histopathologic features associated with response such as TLS, cholesterol clefts, giant cells, and neovascularization were rarely present in pre-treatment biopsies**, Table S1**. Pre-treatment cases tended to have low density TIL, with high TIL density scores only seen in post-treatment cases (p=0.11 and 0.023, respectively). When the pre-treatment specimens from patients with subsequent MPR (n=7) vs. NR (n=4) were compared, no pre-treatment histopathologic features were significantly associated with response.

Additional histopathologic findings

As shown in Figure 3A, nearly every case that showed some degree of response (<90% RVT) was associated with a moderate to markedly dense infiltrate of immune cells. Patient 11 was one

exception and showed histologic features of immune exclusion, **Figure S4A**. Multiplex IHC/IF was used for spatially-resolved quantification of CD8-positive T cells relative to the tumor-stromal border, highlighting the striking pattern, **Figure S4A and B**.

The specimens from the three patients who had early disease recurrences were reviewed to assess for histologic features following anti-PD-1 therapy that may predict more aggressive clinical behavior**.** Two of the patients that showed disease recurrence were scored as partial pathologic responders, but showed minimal histologic features (Patient 14 and 16 from **Figure 3A)**. The third patient (Patient 6) who recurred demonstrated a cMPR/irMPR in the lung and no evident lymph node metastases in the definitive resection specimen. This patient unfortunately experienced a recurrence in an unresected mediastinal lymph node. This case is notable, as it highlights the potential for a mixed response, even in the neoadjuvant setting.

For patients treated with pre-operative chemotherapy, studies suggest that pCR is more likely observed in those with a squamous histology [8, 9]. A correlation was not observed in this pilot cohort between histologic subtype and response to neoadjuvant anti-PD-1 [7]. Lymph nodes devoid of tumor were also assessed to determine if any features correlated with treatment response. A heterogeneous pattern of reactive changes was observed, however, none correlated with treatment response, **Figure S5**.

Table S1. Summary of differences between the criteria for grading pathologic response to neoadjuvant chemotherapy and immunotherapy.

Property	Chemotherapy Criteria[2, 12]	irPRC
Composition of tumor bed (components sum to 100%)	• RVT • Necrosis • Stromal tissue	• RVT • Necrosis • Regression bed
Definition of 'stromal tissue'	'fibrosis' and 'inflammation'	Tissue area between discrete tumor islands. If features of regression are absent, intratumoral stroma is counted as part of RVT area.
'Inflammation'	Not otherwise specified	Specific cell types are assessed including lymphocytes, giant cells, neutrophils, plasma cells, etc.
'Fibrosis'	Not otherwise specified	Differentiates between new, proliferative fibrosis vs. established, mature fibrosis
Calculation of final %RVT score for primary tumor specimen	%RVT is determined for each slide individually, and then averaged across slides containing tumor (weighs each slide equally)	%RVT is determined by summing tumor area and tumor bed area across all slides containing tumor (weighs slides by amount of tumor on each)
Lymph node assessment	Limited by requirement of pathologically-confirmed nodal disease at initial diagnosis. Scoring of specific histologic features not described.	Same as for primary tumor. Regression bed can be recognized in absence of residual viable tumor.
Regression bed	N/A	Region(s) of the radiographically and grossly identifiable "tumor mass" that have been replaced by proliferative fibrosis with neovascularization and evidence of immune activation and cell death (following immune-mediated tumor regression)

Table S2. Pathologic features in paired pretreatment samples versus PD-1 blockade treated specimens

Feature, n (%)[a]	Pre (n=17)	Post (n=17)	p value[b]
Lymphoid aggregates	3 (18)	16 (94)	0.00087
Fibrosis			
% Fibrosis, Median (range)	0 (0-30)	30 (0-96.5)	0.0021 [c]
Proliferative Fibrosis	3 (18)	8 (47)	0.18
Mature Fibrosis	0 (0)	2 (12)	0.48
Mixed Fibrosis	0 (0)	3 (18)	0.25
Foamy macrophages			
Alveolar	1 (5.9)	12 (71)	0.0026
Interstitial	0 (0)	4 (24)	0.13
Cholesterol clefts	0 (0)	8 (47)	0.013
Tertiary lymphoid structures	0 (0)	8 (47)	0.013
Giant cells	1 (5.9)	9 (53)	0.013
TIL score			
Low (1+)	11 (65)	5 (29)	0.11
High (3+)	0 (0)	7 (41)	0.023
Neovascularization	1 (5.9)	10 (59)	0.016
Dense plasma cells	2 (12)	9 (53)	0.023
Granulomas	0 (0)	4 (24)	0.13
Hemosiderin	3 (18)	6 (35)	0.37
Necrosis	4 (24)	8 (47)	0.22
Neutrophils	5 (29)	6 (35)	1

[a]All features are reported as n(%) of patients with the feature present, unless otherwise noted.
[b]McNemar's test, unless otherwise noted.
[c]Student's t-test

Table S3. Case Report Form for Pathologic Response after Neoadjuvant Immunotherapy

Neoadjuvant Lung Case Review

Subject ID Number _____

Case Number _____

Total number of slides examined _____

Review date _____

Tumor Information

Percent of total tumor bed with viable tumor _____

Percent necrosis in total tumor bed _____

Percent fibroinflammatory stroma/regression in tumor bed _____ =100%

Tumor Immune Pattern

Tumor immune patterning
- ◯ No significant immune infiltrate
- ◯ Immune excluded
- ◯ Immune infiltrated
- ◯ Separate foci showing immune exclusion and infiltration

Tumor immune patterning comments _____

Focality (microscopically) of malignant cells within individual tumor bed
- ◯ Unifocal
- ◯ Multifocal

If multifocal, number of microscopic foci of malignant cells within individual tumor bed _____

Tumor Response

Major pathologic response (≤10% residual viable tumor)
- ◯ Yes
- ◯ No
- ◯ N/A

Complete pathologic response (0% residual viable tumor)
- ◯ Yes
- ◯ No
- ◯ N/A

Lymph Node Information

Number of lymph nodes examined _____

Number of lymph nodes positive _____

Features of tumor regression present in lymph node
- ○ Yes
- ○ No

If yes, number of nodes with regression _____

Percent of total tumor bed with viable tumor _____

Percent necrosis in total tumor bed _____

Percent fibroinflammatory stroma/regression in tumor bed _____

=100%

Lymph Node Immune Pattern

Lymph node immune patterning
- ○ No significant immune infiltrate
- ○ Immune excluded
- ○ Immune infiltrated
- ○ Separate foci showing immune exclusion and infiltration

Lymph node immune patterning comments _____

Focality of malignant cells in lymph node
- ○ Unifocal
- ○ Multifocal

If multifocal, number of malignant cell lymph node foci _____

Lymph Node Response

Major pathologic response (≤10% residual viable tumor)
- ○ Yes
- ○ No
- ○ N/A

Complete pathologic response (0% residual viable tumor)
- ○ Yes
- ○ No
- ○ N/A

Figure S1

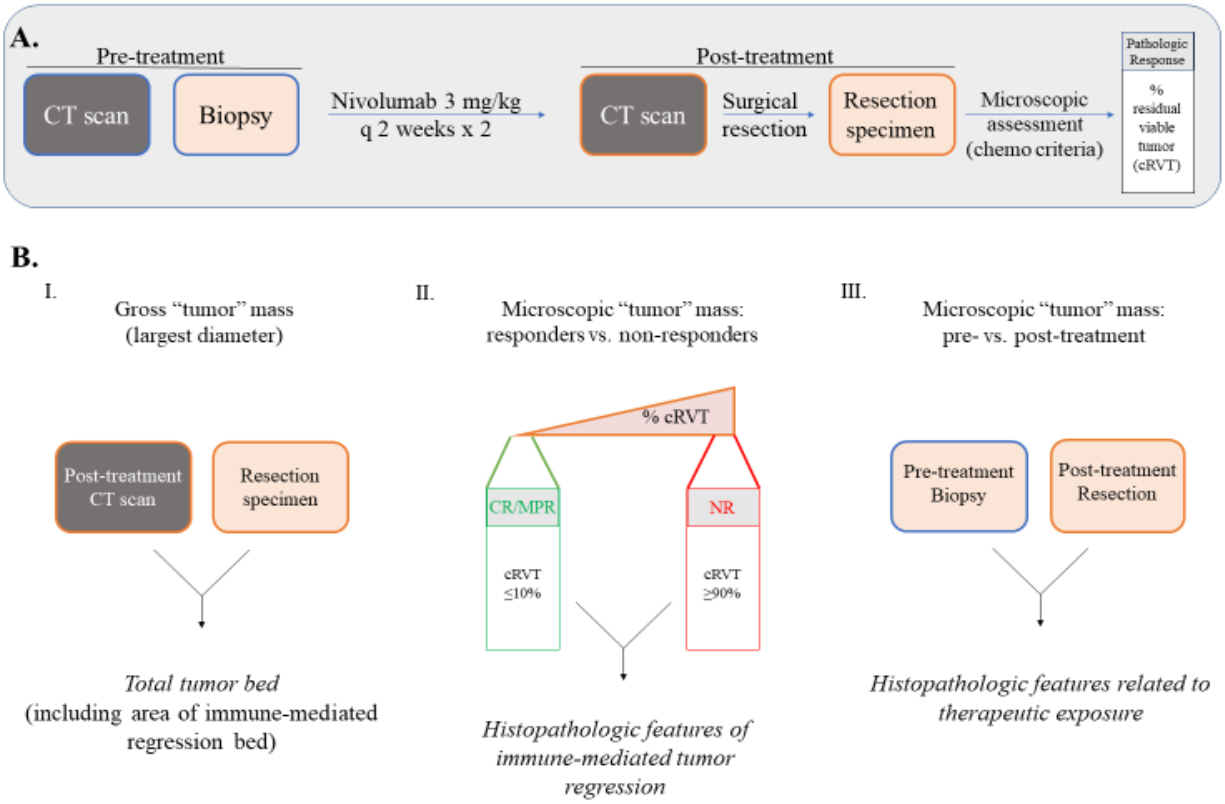

Figure S1. Study overview. (A) The clinical trial enrolled newly diagnosed patients with resectable NSCLC [7]. Patients underwent pre-treatment biopsy and a body CT scan prior to treatment. Patients then received two doses of anti-PD-1 and had repeat chest CT ≤7 days prior to surgical resection. Radiologic responses were classified according to RECIST 1.1 with modifications [11]. Lung resection specimens were evaluated for pathologic response using chemotherapy criteria (cRVT) [2]. All resections included regional lymph nodes, with a median 18 nodes removed per patient (range 5-36). 9/20 patients had lymph node metastases at the time of resection. **(B)** The current study further evaluates immune mediated pathologic response via (I) Comparison of the greatest "tumor" mass dimension on post-treatment CT scan vs. the gross resection specimen to define the total tumor bed (including residual tumor and regression); (II) Microscopic identification of histopathologic features of response via comparison of complete and major pathologic responders (CR/cMPR, ≤10% cRVT) to non-responders (NR, ≥ 90% cRVT); and (III) Microscopic evaluation of pre-treatment core needle biopsies (n=17 were available) for histopathologic features predictive of, or associated with, major pathologic response. For patients with multiple pre-treatment biopsies (n=1 with three; n=5 with two), the specimen with the greatest amount of tumor present was chosen for further assessment. The median time between pre-treatment specimen procurement and treatment initiation was 25 days (range 6 - 92 days).

Figure S2

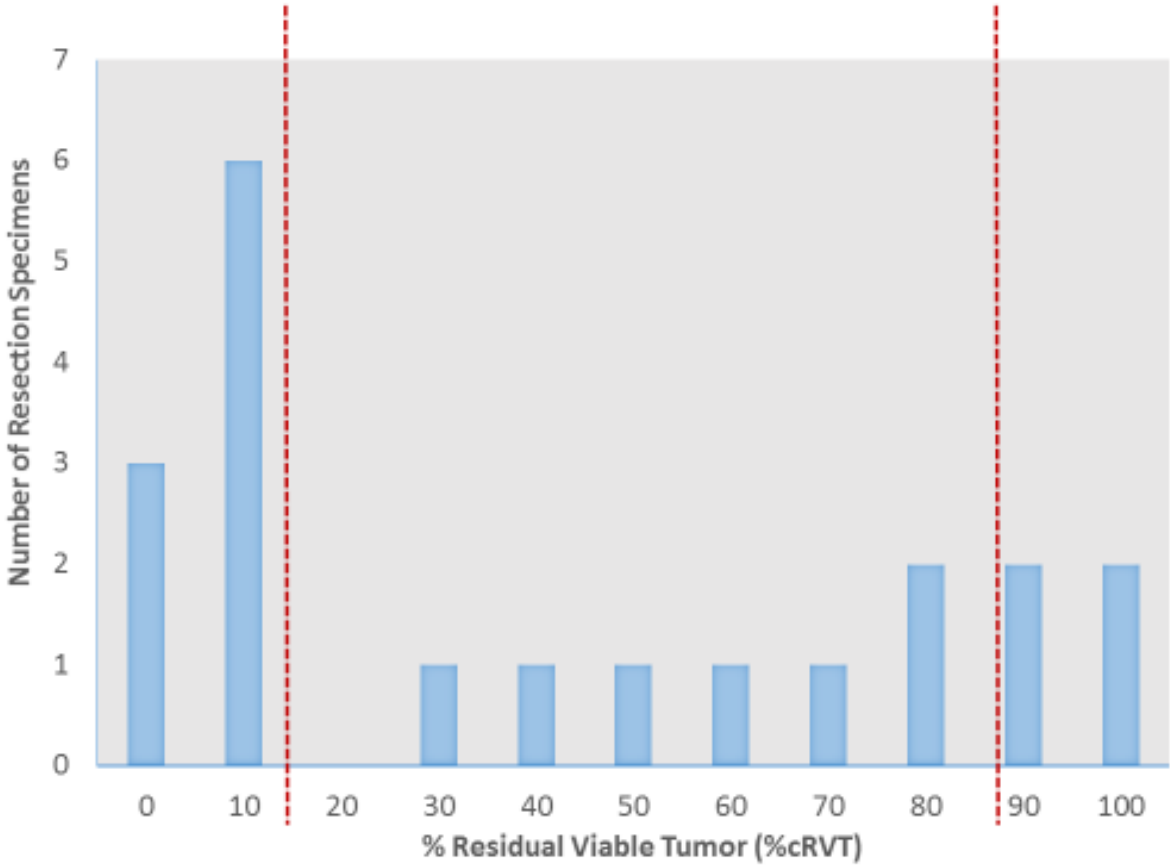

Figure S2: Histogram showing distribution of %cRVT in lung resection specimens. The two extremes of the cohort (≤10% RVT and ≥90% RVT, shown by red dotted lines and considered major pathologic responders/complete pathologic responders and pathologic non-responders, respectively) were compared to identify candidate histologic features associated with immune-mediated tumor clearance. One of the three complete pathologic responders shown in the histogram had no RVT in the lung, but had residual tumor present in lymph nodes.

Figure S3

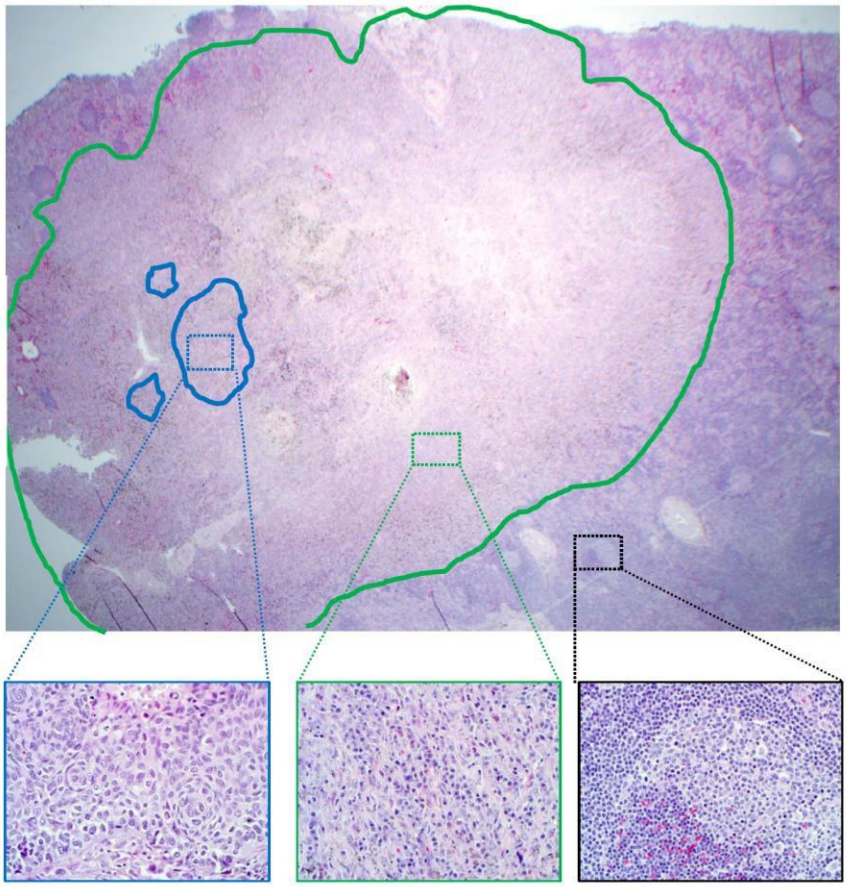

Figure S3: irPRC can potentially be applied to lymph nodes from definitive surgical resection specimens. Example above shows regression bed (neovascularization, proliferative fibrosis, plasma cells and hemosiderin highlighted by green circle) and residual tumor (blue circles) replacing a normal lymph node (normal germinal center shown in black square). By irPRC, this lymph node would be scored as ≤10% irRVT, *i.e.* irMPR. We propose that multiple tumor deposits and/or regression beds in lymph nodes are handled similarly to the primary lung tumor, so that % irRVT = total tumor burden in the assessed lymph nodes. Analyses of the clinical significance of these two locations can then be conducted for each of these locations separately and also combined. Original magnification of 20x, with higher power regional views at 400x.

irPRC has superior resolution to the lymph node component of the current AJCC staging and the chemotherapy neoadjuvant calculation for 'residual tumor burden calculator' [12], both of which tally the number of lymph nodes involved by tumor and the greatest dimension of the largest tumor deposit, because the irPRC provides a metric of whether any immune-mediated clearance at this location was achieved. If irPRC is shown to be a reproducible metric for scoring lymph node involvement, the limitation for assessing nodal disease then reverts to a sampling issue, as exemplified by Patient 5 who demonstrated a complete pathologic response in the lung tumor and showed no pathologic evidence of lymph node involvement in sampled nodes, yet progressed/relapsed in unsampled mediastinal lymph node disease.

Figure S4

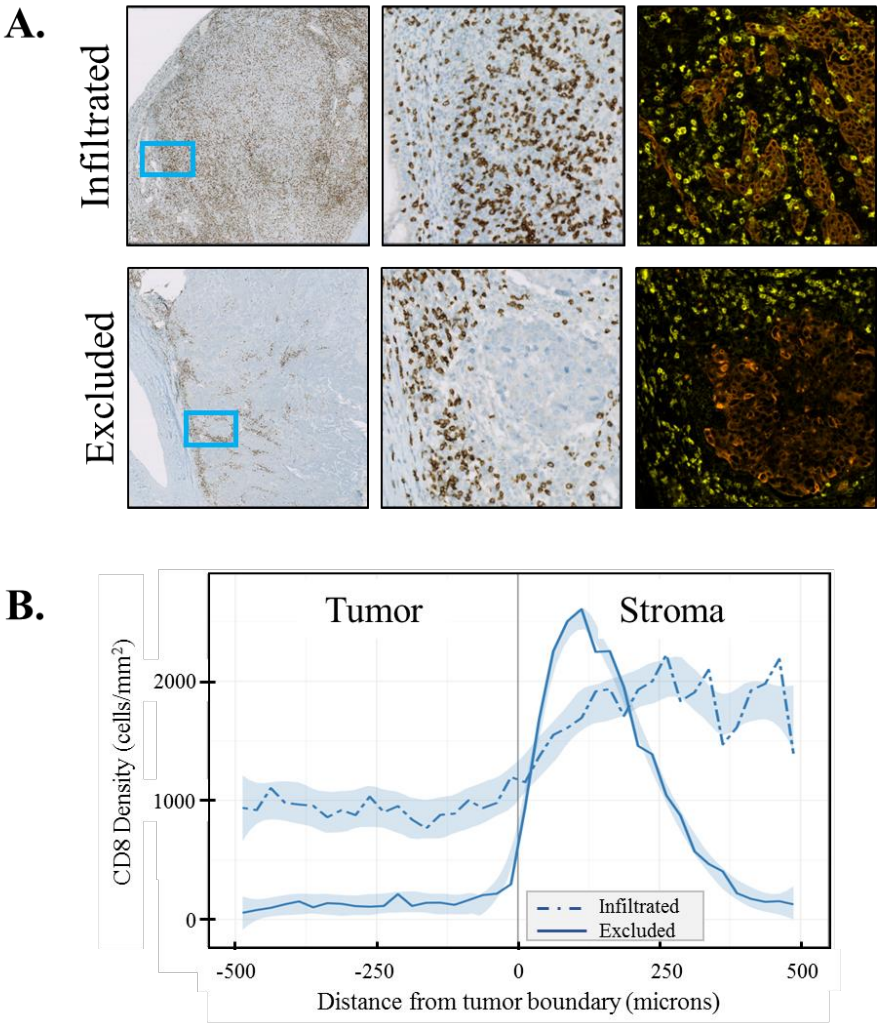

Figure S4. Patterns of both immune infiltration and immune exclusion were evident in the residual viable tumor in specimens from partial responders. (A) Top row: Low power (left panel) and high-power (middle panel) CD8 immunostain photomicrographs from Patient 12 showing dense and diffuse immune infiltration of post-treatment tumor by CD8+ T cells. Bottom row: low power (left panel) and high-power (middle panel) CD8 immunostain photomicrographs from Patient 11 showing CD8+ T cells densely concentrated in the immediate peritumoral stroma and virtually absent within the tumor mass, consistent with an immune exclusion pattern. Right panels: Multiplex IF highlights the contrasting patterns of CD8+ T cells (yellow) infiltrating into the cytokeratin (+) tumor (orange) on the top rowvs. being excluded from the tumor on the bottom row. **(B)** Spatially resolved digital quantification of the multiplex IF images shows the high density of intratumoral CD8+ cells in the infiltrated tumor (dashed line) relative to the paucity of intratumoral CD8+ T cells in the immune excluded tumor (solid line).

Figure S5

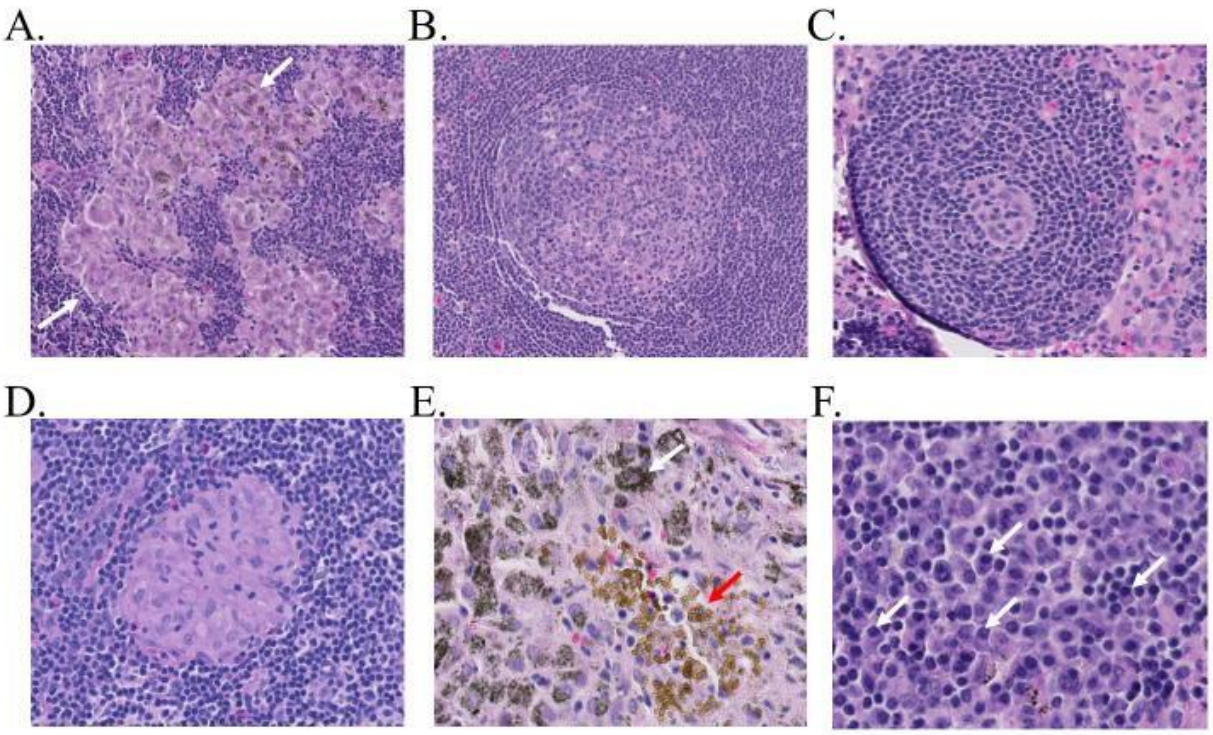

G.

	cMPR (n=8)	cPR (n=7)	cNR (n=4)	Total (N=19)
Follicular Hyperplasia	5 (63)	6 (86)	4 (100)	15 (79)
Sinus histiocytosis	7 (88)	5 (71)	3 (75)	15 (79)
Granulomas	7 (88)	4 (57)	3 (75)	14 (74)
Plasmacytosis	1 (13)	3 (43)	1 (25)	5 (26)
Castleman-disease like changes	1 (13)	1 (14)	0 (0)	2 (11)
Hemosiderin	4 (50)	4 (57)	2 (50)	10 (53)

cMPR=≤10% cRVT; cPR = >10% but < 90% cRVT; cNR ≥ 90% cRVT

Figure S5: Histopathologic features in non-tumor bearing lymph nodes after two doses of anti-PD-1 therapy. These features included: (A) sinus histocytosis (arrows). In some cases, the aggregates of histiocytes extend into the paracortex; (B) follicular hyperplasia; (C) Castleman-disease like changes (involution of germinal centers with a prominent, concentric mantle zone), (D) sarcoid-like granulomas, (E) hemosiderin pigment (golden brown, red arrow, vs. black anthracotic/smoking-associated pigment, white arrow), and (F) plasmacytosis (numerous plasma cells are shown, some highlighted by white arrows). (G) Reactive histologic features in non-tumor bearing lymph nodes from patients treated with neoadjuvant anti-PD-1 do not differ between responders and non-responders. All patients had lymph nodes with at least one of these reactive changes, and similar changes were seen in multiple nodes from the same patient. Many of these features may be observed in thoracic lymph nodes that have not been exposed to immunotherapy. They will need to be distinguished from features of pathologic response and other disease processes, *e.g.* granulomas and plasma cells associated with an infectious or autoimmune disease. The majority of the patients who had pre-treatment lymph node sampling had fine needle aspirates performed, precluding a more formal comparison between pre- vs. post-treatment features in the draining lymph nodes. Panels A,B: 200x original magnification; Panels C-E,:400x original magnification; Panel F: 600x original magnification

Figure S6

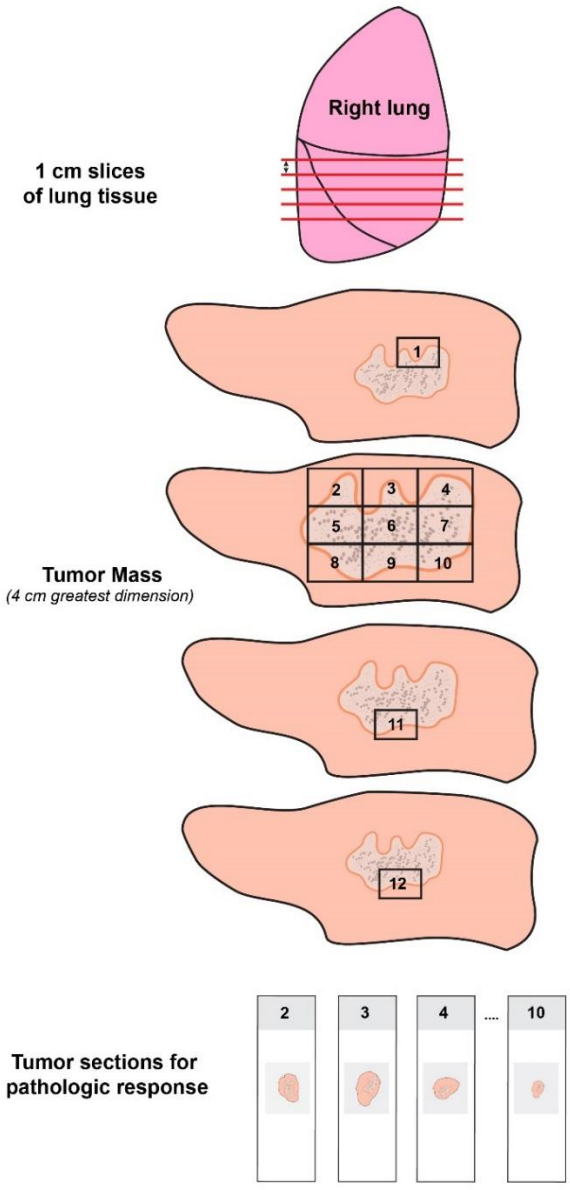

Figure S6: Schematic diagram showing recommended surgical pathology grossing protocol for specimens from patients treated with neoadjuvant anti-PD-1. A complete cross section from the largest diameter of the 'tumor mass' is the most accurate way to quantitate %irRVT. In addition, a section from each additional 1 cm of greatest tumor dimension is recommended, per standard grossing protocols. For example, the figure shows a 4 cm tumor mass, so in addition to the complete cross-section representing 1 cm of tumor that is submitted in cassettes 2-10, three additional single cassettes are also submitted, each representing one of the remaining 3 cm of tumor. In cases of suspected MPR/pCR, the whole "tumor mass" may need to be submitted for histologic examination. A similar approach to grossing has already been recommended for the grossing of breast tumors from patients treated with neoadjuvant chemotherapy.[13]

SUPPLEMENTAL REFERENCES

1. Goldstraw P, Chansky K, Crowley J et al. The IASLC Lung Cancer Staging Project: Proposals for Revision of the TNM Stage Groupings in the Forthcoming (Eighth) Edition of the TNM Classification for Lung Cancer. Journal of Thoracic Oncology 11: 39-51.
2. Pataer A, Kalhor N, Correa AM et al. Histopathologic response criteria predict survival of patients with resected lung cancer after neoadjuvant chemotherapy. J Thorac Oncol 2012; 7: 825-832.
3. Rose BS, Winer EP, Mamon HJ. Perils of the Pathologic Complete Response. J Clin Oncol 2016; 34: 3959-3962.
4. Yamane Y, Ishii G, Goto K et al. A novel histopathological evaluation method predicting the outcome of non-small cell lung cancer treated by neoadjuvant therapy: the prognostic importance of the area of residual tumor. J Thorac Oncol 2010; 5: 49-55.
5. Liu-Jarin X, Stoopler MB, Raftopoulos H et al. Histologic Assessment of Non–Small Cell Lung Carcinoma after Neoadjuvant Therapy. Modern Pathology 2003; 16: 1102.
6. Taube JM, Anders RA, Young GD et al. Colocalization of inflammatory response with B7-h1 expression in human melanocytic lesions supports an adaptive resistance mechanism of immune escape. Sci Transl Med 2012; 4: 127ra137.
7. Forde PM, Chaft JE, Smith KN et al. Neoadjuvant PD-1 Blockade in Resectable Lung Cancer. N Engl J Med 2018.
8. Mouillet G, Monnet E, Milleron B et al. Pathologic complete response to preoperative chemotherapy predicts cure in early-stage non-small-cell lung cancer: combined analysis of two IFCT randomized trials. J Thorac Oncol 2012; 7: 841-849.
9. Liao WY, Chen JH, Wu M et al. Neoadjuvant chemotherapy with docetaxel-cisplatin in patients with stage III N2 non-small-cell lung cancer. Clin Lung Cancer 2013; 14: 418-424.
10. Hellmann MD, Chaft JE, William WN, Jr. et al. Pathological response after neoadjuvant chemotherapy in resectable non-small-cell lung cancers: proposal for the use of major pathological response as a surrogate endpoint. Lancet Oncol 2014; 15: e42-50.
11. Eisenhauer EA, Therasse P, Bogaerts J et al. New response evaluation criteria in solid tumours: revised RECIST guideline (version 1.1). Eur J Cancer 2009; 45: 228-247.
12. Symmans WF, Peintinger F, Hatzis C et al. Measurement of residual breast cancer burden to predict survival after neoadjuvant chemotherapy. J Clin Oncol 2007; 25: 4414-4422.
13. Provenzano E, Bossuyt V, Viale G et al. Standardization of pathologic evaluation and reporting of postneoadjuvant specimens in clinical trials of breast cancer: recommendations from an international working group. Mod Pathol 2015; 28: 1185-1201.